Seismic Performance of Wall-stud Shear Walls

Ludovic A. Fulop

Dan Dubina

Sixteenth International Specialty Conference on Cold-Formed Steel Structures
Orlando, Florida USA, October 17-18, 2002

Seismic Performance of Wall-Stud Shear Walls

Ludovic A. Fulop[1], Dan Dubina[2]

Abstract

The ever-increasing need for housing generated the search for new and innovative building methods to increase speed, efficiency and enhance quality, one direction being the use of light steel profiles as load bearing elements and different materials for cladding. Wind and seismic behavior of these structures is influenced by the hysteretic characteristics of the shear wall panels. In this paper a review of actual research in the field and results of a full-scale shear test program on wall panels are presented. Based on tests, a numerical equivalent model for hysteretic behavior of wall panels working in shear was built to be used in 3D dynamic nonlinear analysis of cold-formed steel framed buildings.

Introduction

Steel-framed houses are usually built of light cold-formed steel load bearing structure and having different solutions of interior and exterior cladding. This technology is popular and accounts for an important and ever increasing market share, especially in the US, Japan, Australia and Europe (Pekoz 1995). The same method is used for small buildings, of other purposes (offices, schools, manufacturing premises, etc.), that are referred as Small Industrial Buildings (SIB).

In such structures shear walls are the main structural elements to act against horizontal loads, e.g. wind and earthquake. Even if widely used in practice, behavior of shear walls subjected to earthquake is not fully understood and in recent years important effort has been made to clarify certain aspects related to shear wall strength, stiffness and ductility.

Literature review of recent research results

Research in the US (AISI 1997, Serette 1996, Salenicovich 2000) has been focused mainly towards experimental testing of shear walls typical to their home practice, in order to produce

[1] PhD Student, Department of Steel Structures and Structural Mechanics, Civil Engineering and Architecture Faculty, "Politehnica" University of Timisoara, Ioan Curea st. 1, Timisoara RO-1900, Romania , E-mail: lala@constructii.west.ro

[2] Prof., Department of Steel Structures and Structural Mechanics , Civil Engineering and Architecture Faculty, "Politehnica" University of Timisoara, Ioan Curea st. 1, Timisoara RO-1900, Romania E-mail: dubina@constructii.west.ro

practical racking load values. Load bearing capacities are derived both from monotonic push-over curves, envelope and stabilized envelope curves from cyclic tests. Findings of these studies suggest a conventional elastic stiffness for a wall panel at 0.4 of the ultimate load (Serette 1998). Different frame typologies with various cladding materials were tested, studies being conducted to determine the influence of length/height ratios as well as the effect of openings. Even if very detailed, the majority of studies avoid addressing an important aspect of shear wall behavior, energy dissipation capacity due to cyclic characteristics (Serette 1996). The effect of gypsum wallboard was also studied, leading to the conclusion that both strength and stiffness are increased by the presence of gypsum wallboard, some results suggesting an increase in ultimate load of up to 30%, compared to the case of external sheeting.

Testing and numerical simulation was combined in order to account for hysteretic characteristics in an attempt to provide evidence on the possible values of response modification factors (q) (Kaway 1999). Vibration tests of steel-framed houses were conducted and relatively large damping ratios were found due to interior and exterior finishes. According to the tests damping ratio of 6% was accepted for seismic analysis. A maximum 1/50 rad story drift angle limit is also suggested as acceptable during severe earthquakes. In the Finite Element (FE) analysis stage, a steel-framed house was subjected to two levels of seismic waves. The house exhibited good performance, reaching a maximum drift of 1/300 rad. Even when minimum required wall length was provided, the maximum drift did not exceed 1/60 rad.

The same issue is analyzed by Gad (Gad & all. 2000, Gad 1999), who proposes a new analytical approach to evaluate the ductility parameter (R_{μ}), and finds a value between 1.5 and 3.0 to be suitable. The same research briefly assesses inherent structural overstrength and finds it to be very important factor as far as earthquake resistance is concerned. The quantitative evaluation of overstrength is more difficult, but an empirical evaluation attempt is performed in the report. (Gad & all. 2000)

Experimental tests and FE modeling was employed by G. de Matteis (1998) to assess shear behavior of sandwich panels both in single story and multi-story buildings. A number of six monotonic and six cyclic tests were performed on full-scale sandwich panel specimens of different configurations. In the final stage of the study, dynamic modeling on panels integrated in building structures, under real earthquake records is performed. According to the conclusions diaphragm action can replace classical bracing solutions only in low-rise buildings, and in areas of low seismicity. For multi-story frames cladding panels can only be used in an integrated system, sharing horizontal force with frame effect.

Description of the experimental program

The experimental program was based on six series of full-scale wall tests with different cladding arrangements based on common practical solutions in both housing and SIB (Table 1). Each series consisted of identical wall panels, tested statically both monotonic and cyclic. The main frame of the wall panels were made of cold-formed steel elements, top and bottom tracks were 600T225-62 (U154/1.5), while studs were 600S175-62 (C150/1.5) profiles, fixed at each end to tracks with two pair SPEDEC SL4-F-4.8x16 (d=3/16 in.) self-drilling self-taping screws. In specimens using corrugated sheet as cladding the sheets were placed in horizontal position, with a useful width of 3-3/4 in. (1035mm) and one corrugation overlapping and tightened with seam fasteners SL2-T-A14- 4.8x20 (d=3/16 in.) at 7-7/8in. (200 mm) intervals (Figure 1.a.). Corrugated sheet was fixed to the wall frame using SD3-T15-4.8-22 (d=3/16 in.) self-tapping screws, sheet ends being fixed in every corrugation (4-1/2 in.), while on intermediate studs at every second corrugation (9 in.). Additionally on the specimens in Series II, ½ in. (12.5mm) thick gypsum panels (4x8ft.) were placed vertically and fixed at 10in. (250mm) intervals on each vertical stud.

Table 1. Description of wall specimens

Series	Opening	Bracing	Exterior Cladding	Interior Cladding	Testing Method	Loading Velocity (cm/min)	No. of Tests
O	-	-	-	-	Monotonic	1	1
I	-	-	Corrugated Sheet LTP20/0.5	-	Monotonic	1	1
					Cyclic	6 – 3	2
II	-	-	Corrugated Sheet LTP20/0.5	Gypsum Board	Monotonic	1	1
					Cyclic	6 – 3	2
III	-	Yes	-	-	Monotonic	1	1
					Cyclic	3	1
IV	Door	-	Corrugated Sheet LTP20/0.5	-	Monotonic	1	1
					Cyclic	6 - 3	2
OSB I	-	-	10 mm OSB	-	Monotonic	1	1
					Cyclic	3	1
OSB II	Door	-	10 mm OSB	-	Monotonic	1	1
					Cyclic	3	1

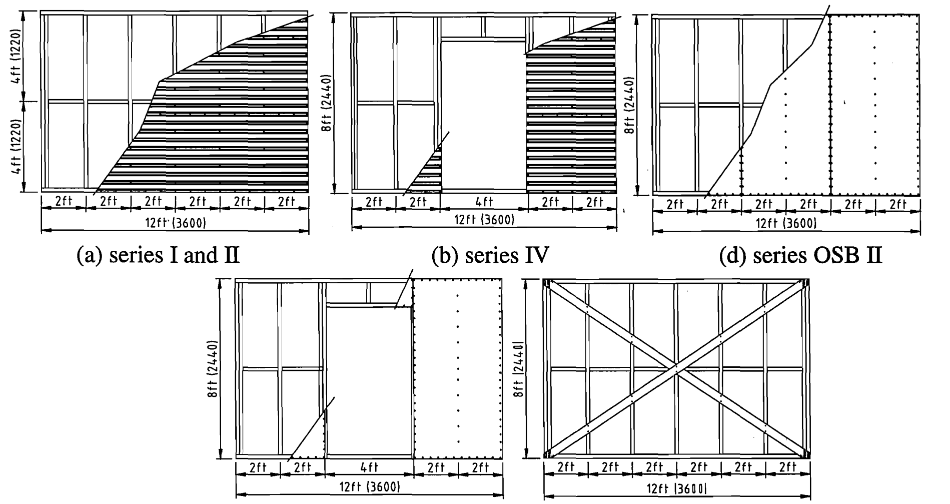

(a) series I and II (b) series IV (d) series OSB II

(c) series OSB I (e) series III

Figure 1. External sheeting configuration of wall specimens

Bracing was used in three specimens (Figure 1.b), by means of 4-3/8in.x1/16in. (110x1.5 mm) straps on both sides of the frame. Steel straps were fixed to the wall structure using SPEDEC SL4-F-4.8x16 (d=3/16in) and SD6-T16-6.3x25 (d=1/4in.) self-drilling screws, the number of screws being determined to avoid failure at strap end fixings and facilitate yielding. 3/8 in. (10mm) OSB panels (4ftx8ft. or. 1200x2440mm) were placed in similar way as the gypsum panels in earlier specimens (Figure 1.d.e), only on the 'external' side of the panel and fixed to the frame using bugle head self-drilling screws of 3/16in. (4.2mm) diameter at 4-1/8in. (105 mm) intervals.

The full-scale testing program was completed with tensile tests to determine both material properties for components and behavior of connections.

Test procedure

For the experiments the testing frame at the University of Timisoara, Department of Steel Structures and Structural Mechanics, equipped with two actuators of 224.8kip (1000kN) and 112.4kip (500kN), was used. The elastic shear force capacity, based on preliminary calculations was evaluated to be at 0.9-1.1kip (4-5kN), and a maximum shear capacity of about 1.8-2.2kip (8-9kN) was expected. Experiments were conducted using displacement control, at the same time measuring the corresponding load with load cell (Figure 2)

Specimens were fixed to a supplementary bottom track (SBT) by means of 7 bolts placed in the vicinity of each stud. In order to increase contact surface supplementary plates were used at each bolt. Corners were further restrained using U profiles instead of the plates, therefore providing increased capacity and rigidity. The specimens were connected to a supplementary upper track in a similar way.

The horizontal load developed by the actuator (A) was transmitted to the specimen via a vertical column (VC), connected to the supplementary top track (STT) by a sliding hinge (SH) with possibility of vertical displacement and load cell (LC). Specimens were loaded in shear very similarly like in earthquake or wind conditions, but without taking vertical loads into account. Specimens were restrained against lateral displacement in two points on the upper part (HSR), which acted as sliding restraint. Displacement transducers were used to measure horizontal displacements (H1, H2) at the top of the specimen, horizontal (H3, H4) and vertical (V1, V2) displacement at the bottom. (Figure 2)

The experimental program was expected to provide information on: comparison between monotonic and cyclic behaviour; confirm earlier findings about the effect of interior gypsum cladding; assess the effect of openings; comparison between wall panels with different cladding materials and cross bracing; provide experimental information for the calibration of FE models

A monotonic test using a loading velocity of 0.39in./min (1cm/min), was performed for each type of panel followed by one or two cyclic tests. (Figure 3) Based on the results, initial stiffness (K_o) and conventional elastic limit (e_l) was determined using Method I (Figure 4.a.) The conventional elastic limit displacement (e_l) was used to determine the displacement amplitudes for the cyclic tests. Cyclic testing methodology followed ECCS Recommendation (ECCS 1985), consisting of cycled of $\frac{1}{4}e_l$, $\frac{1}{2}e_l$, $\frac{3}{4}e_l$, $1e_l$, $2e_l$, $2e_l$, $2e_l$, $4e_l$, $4e_l$, $4e_l$, $6e_l$, $6e_l$, $6e_l$,…, until failure or a significant decrease of load bearing capacity. Loading velocity for the cyclic experiments was 6 min/cycle for one specimen and 3min/cycle for the second.

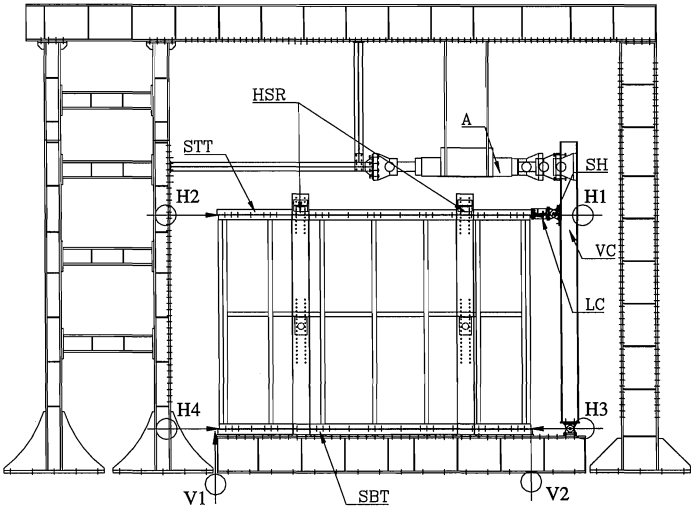

Figure 2. Experimental arrangement

Behavior of specimens

SERIES 0 - Specimen FN-1

For understanding the behavior of sheeted specimens it was important to evaluate initial properties of the skeleton without sheeting, which resulted to have very low capacity and rigidity values. After higher starting value, the rigidity of the panel dropped to 0.07 lbf./in. (12.2N/mm), and load-bearing capacity reached the value of about 224.8 lbf. (1000N).

SERIES I - Specimen I-1, I-2, I-3

One specimen was tested monotonically and two cyclically. Based on the findings from specimen I-1 the e_l has been determined using Method I as being 3/4in. (19.28 mm) corresponding to a force level of F=10581 lbf. (47066.7N). Damage was initiated in the lower uplifted corner, where important deformation of the bottom track occurred. As displacement was increased profile-end distortion of the corrugated sheets was observed on both end studs of the panel. Local deformation of connections has gradually developed especially in the two horizontal seams and in their vicinity. Failure of the specimens occurred in one of the seams, where most of the plastic deformation concentrated. After failure of the seam, sheeting to frame connections closest to the seams continued to provide load bearing capacity. The 'unzipping' of the vertical connecting lines continued as load bearing capacity decreased and in some cases at the final stage local deformation (buckling) of the studs was also observed.

SERIES II – Specimen II-1, II-2, II-3

Panels identical to that in Series I (with corrugated sheeting) were placed in the rig, and supplementary gypsum board was applied to the 'inner' side of the panel. Based on the monotonic curve e_l was evaluated to be 0.6 in. (15.05 mm). The steel skeleton and the 'outer' corrugated sheet had similar behavior as for specimens in Series I. Local deformation in the uplifted corners was followed by profile-end distortion, gradual deformation in connections and failure occurred in seam lines as earlier observed. The behavior of gypsum panels was found to be satisfactory. Panels were not destroyed, but they could follow even extreme deformation of the wall without significant damage. The damage that appeared at low displacement was due to relative vertical slip of the gypsum panels and consecutive crack of the gypsum panel 'seams'. Damage in vicinity of screwed connection, especially pulling trough screw head, was observed at higher displacement levels. Damage was found to be easily reparable without the replacement of gypsum panels, by supplementary fixings and repainting.

SERIES III - Specimen III-1, III-2

Specimens have been manufactured using strap bracing on both side of the frame. The intention was to assure failure of the specimen due to yielding, avoid premature failure in end region of straps and ensure high level of ductility. After buckling of compressed straps in the early stage, the local deformation of the lower track followed, and the damage concentrated entirely in the corner area. After important deformation of corner there were some signs of connection elongation, and redistribution of load to the second and third stud. Important plastic elongation of the straps was observed, but because of this unexpected failure of the corner, it is important to note that results may not conclusively reflect the capacity and ductility expected from strap braced wall panels.

SERIES IV – Specimen IV-1, IV-2, IV-3

Three specimens were prepared with door opening and based on monotonic experiment e_l was evaluated to 15/16in. (23.5mm) with corresponding force level of F=7531lbf. (33500N). Behavior of specimens was very similar to the ones in Series I and Series II, with some particularities. The tendency of corner lift-up was much stronger in comparison to specimens from Series I and II. In lesser extend the uplift phenomenon was observed in the vicinity of the studs around the opening. In the lintel area deformation patterns suggested strong shear effect followed by important local buckling of the corrugated sheet. End profile distortion was present on lateral studs and in the vicinity of opening. Gradual deformation of the screwed connections ended in failure of one of the lower (un-continuous) seams. While load=bearing capacity was already decreasing, unzipping of the corrugated sheet from studs, both lateral and near the opening occurred.

SERIES OSB I – Specimen OSB I-1, OSB I-2

In this case failure mechanism of the specimen was different from corrugated sheet specimens due to different sheeting arrangement. e_l was determined to be 3/4in. (19.2mm), and the cyclic specimen was tested according. Due to increased load bearing capacity uplift effect induced in the corner detail was more important. The three OSB panels placed vertically produced rigid body rotations during deformation and difference of deformation between panel and skeleton had to be accommodated by the screws. This led to important deformation of the fixing screws and relative vertical slip of one OSB panel to the other. Failure of the specimen was sudden when one vertical row of screws unzipped from the stud and both pull over the screw head, and failure of OSB margins was observed.

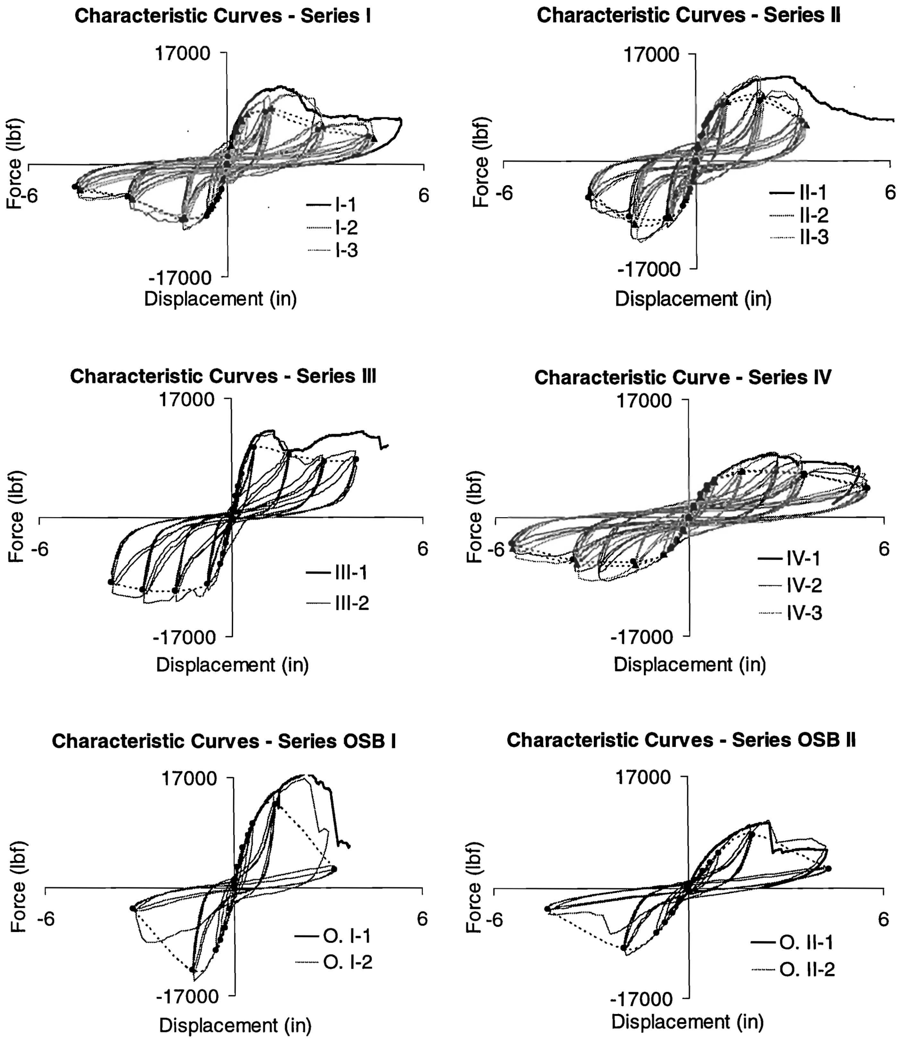

Figure 3. Experimental curves for all specimens

SERIES OSB II – Specimen OSB II-1, OSB II-2

One monotonic and one cyclic specimen were included in this series, and e_l was determined to be 1in. (25.7mm). Loading history was derived based on the e_y value. Uplift deformation was observed in the tensioned corner and for lesser extend in the vicinity of studs near opening and local crushing of OSB in the lintel area was also noted. Important inclination of the screws developed in the screws connecting OSB panels to the lower track, followed by sudden rupture of this connection line.

Analysis of experimental results

The main outputs of the experiments were shear force versus horizontal displacement at the top of the wall-specimens. Furthermore, horizontal slip at the base of the wall and uplift displacement was measured in the two corners. As in case of the panels clad with corrugated sheet the seams govern the failure, relative slip between two steel sheets was also recorded. Load versus lateral displacement curves are presented for all tested specimens (Figure 3), and in order to illustrate monotonic to cyclic results, stabilized envelope curves are being also presented for the cyclic curves.

As seen wall-panels exhibited very complex, and highly non-linear behaviour. In order to evaluate specific properties like elastic modulus, ultimate force or ductility curves have been interpreted according established procedures:

Method I - Initial stiffness was determined as secant stiffness to the load level of 0.4 F_{max}. The evaluation of the conventional yield limit was based on ECCS Recommendation (ECCS 1985), at the intersection point of the elastic line (K_o) to a line of $0.1K_o$ rigidity, tangent to the experimental curve. Based on this conventional elastic limit (e_l, F_{int}) the ultimate point (F_u, D_u) results at the intersection of the horizontal yield line to the experimental curve in the downloading branch (Figure 4.a.).

Method II - The second method has been reported by Kawai (Kawai & all. 1997). Initial stiffness is defied as the secant stiffness to the point of drift angle corresponding to 1/400 (D_{400}), while the yield line is chosen in a way that the hatched parts in

Figure 4.b. have the same area. The allowable strength is referred as the minimum of the force at story drift angle 1/300 (F_{300}) and 2/3 F_{max}.

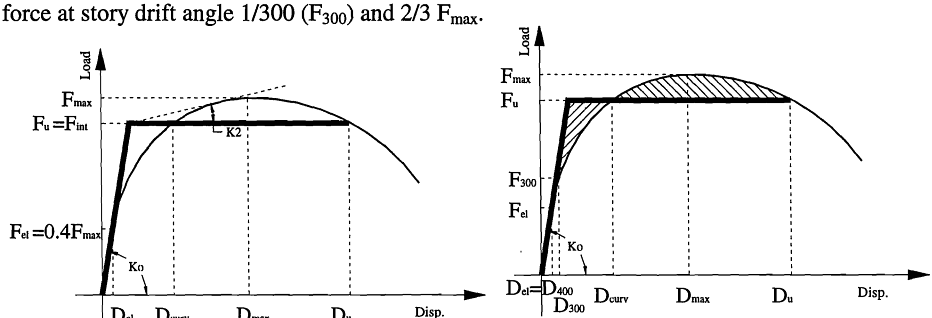

(a) Method I (b) Method II

Figure 4. Methods for determining equivalent elastic-plastic model

Results from monotonic and cyclic experiments are presented (Table 2, Table 3); where two cyclic tests were performed the values are based on the mean value of the two. For cyclic tests, values are derived based on 1st envelope curve (envelope curve), and the 3rd envelope curve (stabilized envelope).

The two methods usually yield similar results, with interesting particularities. Initial rigidity values are very similar and it is important to realize that, ultimate load (F_u) and ductility are in direct relationship so when a method yields higher ultimate load (F_u) this automatically means lower ductility. For design capacity, the minimum of $2/3F_{max}$ and F_{300} and F_{200} are relevant, since they represent the values accepted in the Japanese and US code respectively (Kawai 1997).

Differences between monotonic and cyclic values can be observed as follows. Initial rigidity is not affected, values of cyclic and monotonic tests range within a difference of less than 20%. The same can be noted for ductility, exception being in case of OSB specimens where ductility is reduced by 10-25% for cyclic results. One important observation concerns ultimate load (F_u), where cyclic results are lower than monotonic ones by 5-10% even if we consider 1st envelope curve. If we take into account stabilized envelope curves, the difference can increase to 20-30%.

Based on medium value of monotonic and cyclic results comparison of different series contribution of opening, gypsum board and other factors can be assessed, with the following conclusions:

Series I - Series II: Differences can be attributed to the effect of the gypsum board. There is an increase of in ultimate load of 16.2% and 17.8% respectively. As far as initial values are concerned (K_o, F_{400}, F_{300}, F_{200}) there seem to be no differences, but ductility is also improved slightly.

Series I – Series IV: There is significant decrease of initial rigidity (60.3% – 53.3%), for a lesser degree of ultimate load (16.4% – 21.0%), but ductility values are essentially unaffected

Series I – Series III: Comparison is more qualitative because of the different sheeting system. There are no differences as fare as initial rigidity is concerned; however an increase of ductility has been expected. This was not possible as failure mode for the strap-braced specimens was not the most advantageous one. Strap braced wall panels have the advantage of stable hysteretic loops, but also the disadvantage of higher pinching than the sheeted ones.

Series I – Series OSB I: Comparison more qualitative, keeping in mind the different wall panel arrangements. Initial rigidity is of similar magnitude, with increase of ultimate load. Failure of OSB specimens under cyclic loading was more sudden than in case of corrugated sheet specimens, where degradation occurs gradually. This is also reflected by the reduced ductility for OSB specimens.

Series OSB I – Series OSB II: The effect of opening produced similar results as in cases of Series I – Series IV. Initial rigidity decreased with 64.6% – 59.1%, while ultimate load decreased with 32.5% - 36.9%. There is also an important decrease of ductility, probably highlighting the different failure modes of the two wall panels.

Table 2. Summary of experimental results, Method I

		K_o - (lbf/in) (N/mm)	**F_{el} (lbf) (N)**	**F_{max} (lbf) (N)**	**F_u (lbf) (N)**	**Ductility**
I	**Mon**	25698 *(4500)*	4621 *(20556)*	11887 *(52876)*	9317 *(41444)*	6.35
	1st C	21203 *(3713)*	4070 *(18105)*	10262 *(45646)*	8287 *(36861)*	7.06
	3rd C				6907 *(30722)*	6.25
II	**Mon**	17933 *(3141)*	5364 *(23861)*	13425 *(59715)*	10366 *(46111)*	6.23
	1st C	22280 *(3902)*	5057 *(22496)*	12911 *(57430)*	10148 *(45139)*	6.32
	3rd C				7968 *(35444)*	7.47
III	**Mon**	23250 *(4072)*	4841 *(21533)*	12398 *(55148)*	10866 *(48333)*	3.17
	1st C	20690 *(3623)*	4608 *(20498)*	12033 *(53524)*	10016 *(44556)*	6.24
	3rd C				9080 *(40389)*	6.04
IV	**Mon**	9383 *(1643)*	3560 *(15838)*	9042 *(40220)*	7444 *(33111)*	4.22
	1st C	8833 *(1547)*	3307 *(14708)*	8485 *(37745)*	7272 *(32347)*	5.37
	3rd C				5770 *(25667)*	6.22
OSB I	**Mon**	19524 *(3419)*	7026 *(31252)*	17710 *(78777)*	14613 *(65000)*	4.14
	1st C	22333 *(3911)*	6071 *(27004)*	15702 *(69844)*	13264 *(59000)*	3.12
	3rd C				11603 *(51611)*	3.18
OSB II	**Mon**	8968 *(1571)*	3968 *(17651)*	9977 *(44380)*	8693 *(38667)*	2.62
	1st C	6884 *(1206)*	3928 *(17471)*	10325 *(45929)*	9617 *(42778)*	1.68
	3rd C				8355 *(37167)*	1.81

Table 3. Summary of experimental results, Method II

		K_o (lbf/in) (N/mm)	**F_{400} (lbf) (N)**	**F_{300} (lbf) (N)**	**F_u (lbf) (N)**	**Duct**	**2/3 F_{max} (lbf) (N)**
I	**Mon**	23344 *(4088)*	5500 *(24467)*	6450 *(28691)*	10751 *(47821)*	4.65	7925 *(35251)*
	1st C	19681 *(3447)*	4617 *(20536)*	5415 *(24087)*	8924 *(39697)*	5.13	6841 *(30431)*
	3rd C				7545 *(33560)*	4.37	
II	**Mon**	18909 *(3312)*	4516 *(20089)*	5474 *(24350)*	12095 *(53801)*	5.03	8950 *(39810)*
	1st C	21988 *(3851)*	5149 *(22904)*	5972 *(26566)*	11022 *(49030)*	5.05	8607 *(38287)*
	3rd C				8952 *(39819)*	5.54	
III	**Mon**	23912 *(4188)*	5647 *(25120)*	7189 *(31980)*	11497 *(51140)*	2.81	8265 *(36765)*
	1st C	20710 *(3627)*	4779 *(21259)*	6060 *(26957)*	10794 *(48014)*	5.25	8022 *(35683)*
	3rd C				9499 *(42252)*	5.02	
IV	**Mon**	9127 *(1598)*	2102 *(9350)*	3085 *(13724)*	7988 *(35533)*	3.79	6028 *(26813)*
	1st C	10086 *(1766)*	2342 *(10416)*	2893 *(12870)*	7479 *(33267)*	5.62	5657 *(25163)*
	3rd C				6028 *(26812)*	6.22	
OSB I	**Mon**	22325 *(3910)*	5350 *(23797)*	6400 *(28470)*	15323 *(68162)*	4.26	11806 *(52518)*
	1st C	23967 *(4197)*	5540 *(24645)*	6507 *(28942)*	12278 *(54615)*	3.88	10468 *(46563)*
	3rd C				11003 *(48945)*	3.67	
OSB II	**Mon**	10363 *(1815)*	2406 *(10702)*	3098 *(13780)*	8321 *(37015)*	3.19	6651 *(29587)*
	1st C	9196 *(1610)*	2138 *(9511)*	2664 *(11850)*	8414 *(37426)*	2.93	6865 *(30539)*
	3rd C				7623 *(33908)*	3.11	

FE model

In order to be able to provide suitable tool for time-history analysis of entire structures the global behavior of the wall panel has to be represented. A very detailed modeling of the panel, based on individual connection behavior could not be sufficiently simple to for this purpose, so modeling had to be simple and efficient on one hand, and accurate on the other. The basic idea is to replace the shear panel with equivalent cross bracing system, a technique often used in elastic calculations for design purposes.

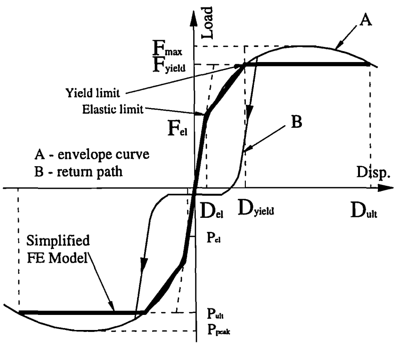

Figure 5. Scheme of hysteretic behavior

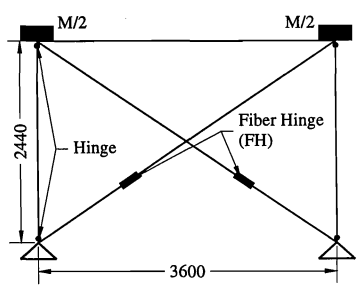

Figure 6. Simplified DRAIN-3DX model

A FE model based on DRAIN-3DX (Prakash and Powell 1993) computer code is proposed in order to get as accurate hysteretic behavior as possible. The simplified model consists of a mechanism frame and a special bracing. As all column ends are hinged the frame itself is a mechanism and does not contribute to load bearing capacity. Braces are modeled as 'TYPE 8' fiber hinge (FH) beam-column elements with FH to accommodate the hysteretic behavior (Figure 6). In order to calibrate the FE model experimental results from a full scale testing program has been used for comparison. (Table 4)

Table 4. Series of FE models and calibrated values based on experimental results

Series	**I**	**II**	**IV**	**OSB I**	**OSB II**
Sheeting	Corrugated Sheet	Corr. Sheet + Gypsum	Corrugated Sheet	OSB	OSB
Initial Rigidity lbf/in. (*N/mm*)	19681 *(3447)*	21988 *(3851)*	10086 *(1766)*	23967 *(4197)*	9196 *(1611)*
Elastic Limit (F_{el}/D_{el}) lbf;in. *(N; mm)*	5415;0.275 *(24086;6.99)*	5972;0.272 *(26566;6.90)*	2893;0.287 *(12870;7.28)*	6506;0.271 *(28942;6.89)*	2664;0.290 *(11850;7.36)*
Yield Limit (F_{yield}/D_{yield}) lbf;in. *(N; mm)*	7545;0.588 *(33560;14.95)*	8952;0.613 *(39819;15.58)*	6028;0.936 *(26812;23.78)*	11003;0.688 *(48944;17.49)*	7623;1.093 *(33908;27.76)*
Ultimate Limit (D_{ult}/Duct) in. *(mm)*	1.678 *(42.61)* /4.37	57.29 *(2.256)* /5.54	94.35 *(3.715)* /6.22	42.85 *(1.687)* /3.67	65.57 *(2.581)* /3.11

Static analysis has been performed and the FE model was exposed to the same lateral displacement history as the experimental wall panels. Comparative experimental to FE curves are presented (for illustrative purposes) (Figure 7) and show good agreement with experimental results, the model being able to account for all important aspects of the experimental curves.

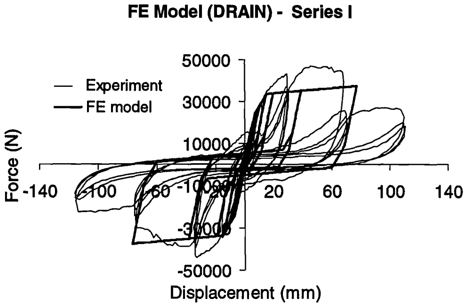

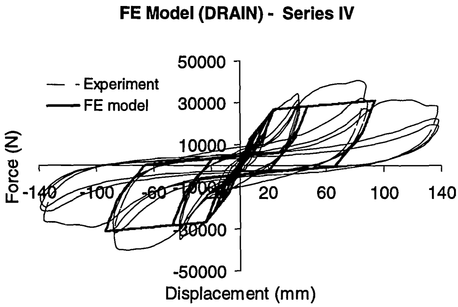

Figure 7. Modeled versus experimental hysteretic curve examples

Testing of the FE model

Being tested through static runs the developed hysteretic model could be used for dynamic time-history analysis. For this purpose the following (Figure 8) earthquake records have been selected. Records have been scaled to Peak Ground Acceleration (PGA) of 1cm/s^2, and elastic spectra with a damping ratio of 5% have been drawn, also comparing them to 'Eurocode 8' (EC8) elastic spectra for A, B and C subsoil conditions (ENV 1998, Eurocode 8). It can be observed that spectra of records resemble reasonably the EC8 elastic spectra, and because they have been scaled to the same PGA, differences of intensity have been largely eliminated.

Using the Single Degree Of Freedom (SDOF) FE model described, time history analysis has been carried out using masses of 2000, 3000, and 4000kg, and records being scaled from 0.05g to 2g. Due to lack or reliable value, damping has not been considered even if values as big as 6% have been suggested at the level of an entire structure (Kano & all. 1999). To account for second order effects a vertical force equal to 30% of the mass value has been also used in the model.

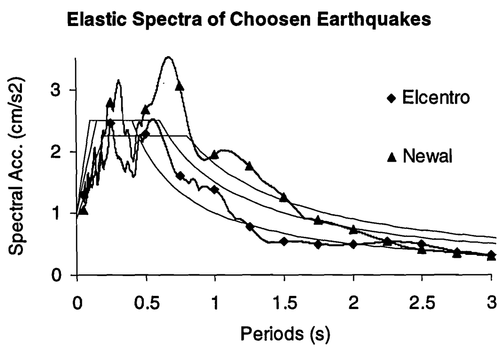

Figure 8. Elastic spectra of records (damp = 5%)

This procedure known as Incremental Dynamic Analysis (IDA) or Dynamic Pushover (DPO) is a common analysis method to more thoroughly estimate structural performance under seismic loads. It is important to note that IDA results are both structure and accelerogram sensitive, therefore large range of accelerograms is recommended.

Primary FE results

Primary results of the numerical simulations are time versus displacement curves and specific hysteretic curves of the model (Figure 9, Figure 10). For the assessment of structural performance an important parameter is top sway displacement during a loading history of an earthquake.

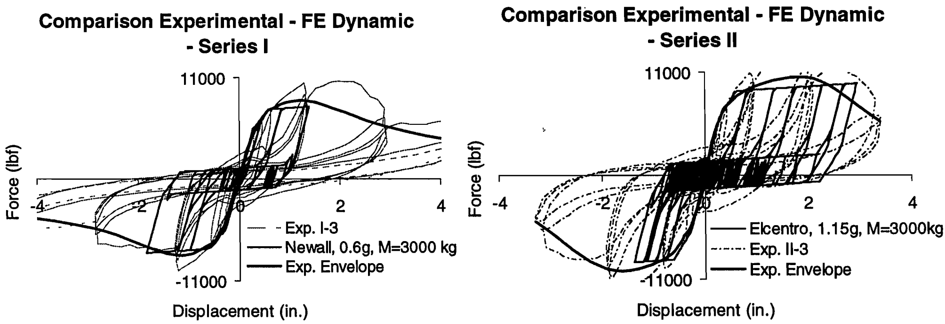

Figure 9. Hysteretic loops during dynamic analysis vs. experiment

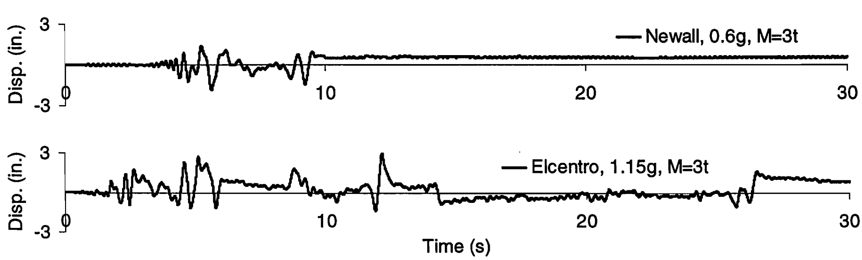

Figure 10. Top-displacement history during earthquake run

More advanced outputs of the analysis consist in IDA curves (Figure 11), relating a performance parameter of the structure to an Intensity Measure (IM) of the record. The IM of the used IDA has to be scalable, PGA, spectral acceleration corresponding to the first mode period of the structure ($S_{a(T1,\beta)}$) or Effective Peak Acceleration (EPA) being the most common ones. Usual structural performance parameters are inter-story drift, maximum plastic rotation, accumulated plastic rotation and top story displacement, depending on the structural typology. Performance parameter can than be related to damage level of the structure and performance based criteria defined to describe the state of the structure after an event of certain intensity.

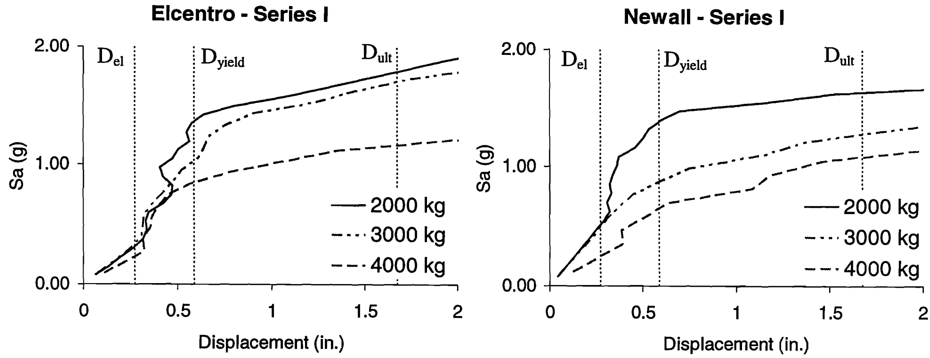

Figure 11. IDA curves for wall panels in Series I

Seismic performance of shear wall panels

Based on the displacement values corresponding earthquake IM levels have been identified for the different panel configurations and earthquake records. The three limit states, identified as vertical lines on the graphs (Figure 11) correspond to the following states; D_{el} – or elastic limit of the panel up to which behavior can be considered elastic and it is the conventional capacity level to be used in design; D_{yield} - yield limit of the wall panel, where the panel lost its load bearing capacity, but it is still capable of deforming under the same load level, D_{ult} – ultimate state, the wall panel is not capable of sustaining a constant load level, and it's capacity is decreasing. Out of this three limit states the last two can be identified fairly accurately, and alternative methods of determination yield similar conclusions. Elastic limit is mostly a conventional value accepted in engineering practice and sometimes very different.

If elastic design is assumed, the limit of L_{el} is the basis of engineering calculations, even if the panels have important post elastic capacities. In seismic design this post-elastic behavior is accounted for by the behavior factor "q" – 'factor used for design purposes to reduce the forces obtained from linear analysis, in order to account for the non-linear response of the structure. (ENV 1998, Eurocode 8) Similarly in US practice "R" is defined as 'response modification factor' or 'system performance factor' that intend to account for damping, energy dissipation capacity and over-strength, and is subdivided in period dependent strength factor R_s, period dependent ductility factor R_μ, and redundancy factor R_R (A. Whittaker, G. Hart, C. Rojahn 1999). As the important effect of structural over-strength has been identified (G. de Matteis & all. 1999), the idea of 'partial q factors' have also penetrated European research in different forms and without any code proposals yet.

As wall panel behavior is highly non-linear and important strength reserve can be identified behind the accepted design allowable strength, it can be expected that over-strength plays an important role in the post-elastic performance. Based on previously defined limit states (D_{el},

D_{yield} and D_{ult}) partial behavior factors can conveniently be defined as ratios of the corresponding IM-s. Following the idea; q_1 has been defined as the ratio of Sa_{el} and Sa_{yield}, and it is primarily a measure of performance due to panel over-strength, while q_2, the ratio of Sa_{ult} and Sa_{yield} is to be understood as performance parameter due to ductility (Table 5).

Table 5. Sa and performance parameters q_1 and q_2

	Series I			Series II			Series IV			Series OSB I			Series OSB II		
M (kg)	**2000**	**3000**	**4000**	**2000**	**3000**	**4000**	**2000**	**3000**	**4000**	**2000**	**3000**	**4000**	**2000**	**3000**	**4000**
Sa_{el} (g)	0.42	0.41	0.24	0.77	0.51	0.31	0.31	0.21	0.18	0.91	0.47	0.35	0.27	0.19	0.12
Sa_{yield} (g)	1.37	0.97	0.75	1.56	1.08	0.80	0.99	0.78	0.66	1.84	1.26	0.92	1.02	0.67	0.59
Sa_{ult} (g)	1.72	1.53	1.13	2.46	1.83	1.45	2.07	1.75	1.29	3.01	1.77	1.29	1.83	1.36	1.22
q_1	3.48	2.42	3.11	2.17	2.17	2.84	3.19	3.80	3.77	2.18	3.04	2.73	3.78	3.80	4.89
q_2	1.25	1.59	1.52	1.58	1.74	1.83	2.17	2.40	1.95	1.64	1.44	1.40	1.81	2.02	2.05
$q_3=q_1 x q_2$	4.40	3.92	4.66	3.53	3.60	5.02	6.73	8.71	7.34	3.72	4.23	3.80	6.84	7.60	9.91
Average	q_1	q_2	q_3	q_1	q_2	q_3	q_1	q_2	q_3	q_1	q_2	q_3	q_1	q_2	q_3
	3.01	*1.46*	*4.35*	*2.48*	*1.68*	*4.13*	*3.42*	*2.12*	*7.10*	*2.68*	*1.42*	*3.78*	*4.07*	*1.90*	*7.69*

It is important to mention that q_1 is highly dependant on the elastic limit defined (D_{el}), limit that is on the other hand conventional. As allowable strength definition was based on 1/300 (Y. Kawai, R. Kano, K. Hanya 1997) story drift angle, for models with low initial rigidity (Series IV and Series OSB II) the criteria is very severe and a very low Sa_{el} is identified. This particularity yields to unrealistically high values of q_1 and q_3 consequently. The value of q_2 instead is less dependent on conventional values, points corresponding to D_{yield} and D_{ult} being more readily definable.

Performance criteria

An important aspect of performance philosophy is to relate lateral displacement to damage and to define acceptable damage levels and relate it to the performance objectives of the panels. Recent performance objective proposals are based on three or four generally stated goals for buildings (FEMA-273 1997): (1) Serviceability under ordinary occupancy conditions; (2) Immediate occupancy following moderate earthquakes; (3) Life safety under design-basis events; (4) Collapse prevention under maximum considered event

Such vague performance criteria can be translated into engineering practice by, for example, relating performance objective to deformations. For lateral loads (ie. wind, earthquake) the inter-storey drift (δ) can be taken as a measure of structural performance as follows; serviceability $\delta<0.005$, immediate occupancy $\delta<0.01$, life safety $\delta<0.05$, collapse prevention $\delta<0.05$.

In case of corrugated sheeting wall panels the main damage is concentrated in seam fasteners. To establish global performance criteria the following acceptable deformations in the seam fasteners can be suggested:

- If slip of the seams does not exceed the elastic limit, corresponding to $0.6F_{max}$ of the seam connection, damage is limited and can be considered negligible. In this case the integrity of the cladding is fully preserved, no repairs are required; it corresponds to serviceability conditions.

- If slip is limited to the diameter of the screw (4.8mm) the cladding requires repair. There is damage, but not excessive and by minor interventions, like replacing screws with larger diameter ones, the structure can be repaired. This could correspond to immediate occupancy.
- In case of life safety criteria any kind of damage is acceptable, without endangering the safety of occupants. This criterion corresponds to the attainment of the ultimate force (F_{ult}) and the starting of the downwards slope.

Relative slip in seams has been measured for specimen I-3, II-2 and II-3 in order to define relevant performance criteria according to previous assumptions (Table 6).

Table 6. Performance criteria

Spec.	Connection Deform. in. & *(mm)*	Force lbf. & *(N)*	Panel Top Disp. in. & *(mm)*	Drift (%)
I-3	0.008 *(0.197)*	4816 *(21423)*	0.26 *(6.71)*	0.274
	1.19 *(4.8)*	9866 *(43885)*	1.15 *(29.22)*	1.197
IV-2	0.008 *(0.197)*	2272 *(10106)*	0.31 *(7.96)*	0.326
	0.008 *(4.8)*	8006 *(35613)*	1.74 *(44.13)*	1.808
IV-3	0.008 *(0.197)*	1989 *(8849)*	0.32 *(8.11)*	0.332
	1.19 *(4.8)*	5920 *(26332)*	1.66 *(42.22)*	1.730

Based on these data the following performance criteria are suggested for wall panels clad with corrugated sheet: (1) fully operational ($\delta<0.003$); (2) partially operational ($\delta<0.015$); (3) safe but extensive repairs required ($\delta<0.025$). Comparable design criteria can be established for other types of panels.

The first performance level does not provide ductility, because shear panel work is limited to elastic domain. This could be the design criteria for frequent, but low intensity earthquakes. In case of rare but severe earthquakes, the last two design criteria can be used and some ductility will be available.

Conclusions

It can be concluded that shear-resistance of wall panels is significant both in terms of rigidity and load bearing capacity, and can be effective against lateral load. The hysteretic behavior is characterized by very significant pinching, and therefore reduced energy dissipation. How this low dissipation affects earthquake performance of the building is to be evaluated.

Failure is usually starting at the bottom track in the anchor bolt region, therefore strengthening of the corner detail is very important. The ideal shape of corner detail is so that uplift force is directly transmitted from the brace (or corner stud) to the anchoring bolt, without inducing bending in the bottom track. Failing to strengthen wall panel corners has important effects on the initial rigidity of the system.

The seam fastener represented the most sensitive part of the corrugated sheeting specimens; damage is gradually increased in seam fasteners, until their failure causes the overall failure of the panel. Much of the post elastic deformation of the panel is in the region of seam fasteners, therefore increasing the load capacity and ductility of the seams will improve the behavior of the panels.

It is very important to underline that in case of all tested specimens the wall stud system proved a very good toughness. Even when damages were very important no collapse occurred. This is of real importance for buildings located in seismic areas. For corrugated sheet specimens, and similarly for others, performance design criteria can be suggested.

Based on experimental evidence a simple FE model has been calibrated to be used in earthquake modeling of shear wall-panels in light structures. The model is accurate enough to take into account all important aspects of the hysteretic behavior and simple enough to be incorporated in more complex structural schemes for full structural modeling. A number of inelastic time-history runs have been performed using different wall panels, acting masses and earthquakes records, and the model has been found satisfactory for the purpose of dynamic analysis.

Using experimentally determined criteria three performance levels were associated with corresponding lateral displacement of the panels and 'partial behavior' factors have been identified for the panels based on time-history analysis results. The effect of over-strength is identified to be important in the post elastic behavior of panels and source of a possible design earthquake-force reduction. The resulting factor (2.2-2.6) is harmonizing reasonably with the value 1.5-5 suggested by Gad & all (1999). The possibility of design force reduction due to ductility and energy dissipation seems to be more limited (1.4-1.6) probably due to low energy dissipation capacity of the hysteretic loops. This value is also in agreement with the findings of Gad & all. (1999).

Reference

AISI (1998). Shear Wall Design Guide, Publication RG-9804, The American Iron and Steel Institute

AISI (1997). Monotonic Tests of Cold Formed Shear Walls with Openings, Prepared by NAHB research Center. Inc., The American Iron and Steel Institute

ECCS. (1985) Recommended Testing Procedure for Assessing the Behaviour of Structural Steel Elements under Cyclic Loads.

ECCS. (1995) European Recommendations for the Application of Metal Sheeting acting as a Diaphragm. Pub.88, European Convention for Constructional Steelwork, Brussels

Eurocode 8. (1998). Design provisions for earthquake resistance of structures

FEMA-273 (1997). NEHRP Guidelines for the Seismic Rehabilitation of Buildings, Prepared by the Building Seismic Safety Council for the Federal Emergency Management Agency, Washington, D.C.

E.F. Gad, A.M. Chandler, C.F. Duffield, G. Hutchinson. (1999). Earthquake Ductility and Overstrength in Residential Structures, Structural Engineering and Mechanics, 8:4, 361-382

E.F.Gad, C.F.Duffield. (2000) Lateral Behaviour of Light Framed Walls in Residential structures, 12 th World Conference on Earthquake Engineering

Gianfranco de Matteis. (1998) The Effect of Cladding in Steel Buildings under Seismic Actions, PhD Thesis, Universita degli Studi di Napoli Federico II

G. de Matteis, R. Landolfo, FM Mazzolani & L. Fulop, D. Dubina. (1999). Seismic response of MR steel frames with different connection behaviours, Proceedings of the 6th International Colloquium SDSS'99, Elsevier, 409-420

Y. Kawai, R. Kanno, K. Hanya. (1997) Cyclic Shear Resistance of Light-Gauge Steel Framed Walls, ASCE Structures Congress, Poland

Y. Kawai, R. Kanno, N. Uno, Y. Sakumoto. (1999) Seismic resistance and design of steel framed houses, Nippon Steel Technical report, No. 79

T. Pekoz. (1995) Building Design Using Cold Formed Sections, Publication of the Swedish Institute of Steel Construction, Stålbyggnadsdagen no. 154

V. Prakash and G. H. Powell. (1994). Drain-3DX Base program description and user guide, Version 1.10, Department of Civil Engineering, University of California at Berkley

A. J. Salenicovich & all. (2000), Racking Performance of Long Steel-Frame Shear Walls, Fifteenth Int. Speciality Conference on Cold-Formed Steel Structures, St. Louis, Missouri, Oct. 19-20, 471-480

R.L. Serette, K. Ogunfunmi. (1996). Shear Resistance of Gypsum-Sheeted Light-gauge Steel Stud Walls, Journal of Structural Engineering, ASCE, 122:4

R.L. Serrette, G. Hall, J. Nygen. (1996) Shear Wall Values for Light Weight Steel Framing, AISI

R.L.Serrette. (1998) Seismic Design of Light Gauge Steel Structures: A discussion, Fourteenth Int. Speciality Conference on Cold-Formed Steel Structures, St. Louis, Missouri, Oct.15-16

Wittaker, G. Hart, C. Rojahn. (1999). Seismic response modification factors, Journal of structural engineering 1999:2, 438-443